This is an *Accepted Manuscript*, which has been through the Royal Society of Chemistry peer review process and has been accepted for publication.

Accepted Manuscripts are published online shortly after acceptance, before technical editing, formatting and proof reading. Using this free service, authors can make their results available to the community, in citable form, before we publish the edited article. We will replace this *Accepted Manuscript* with the edited and formatted *Advance Article* as soon as it is available.

You can find more information about *Accepted Manuscripts* in the **Information for Authors**.

Journal Name

ARTICLE

Conversion of 5-hydroxymethylfurfural into 5-ethoxymethylfurfural and ethyl levulinate catalyzed by MOFs-based heteropolyacid materials

Zhenhua Wang[a] and Qianwang Chen[a,b]

Conversion of 5-hydroxymethylfurfural (HMF) into 5-ethoxymethylfurfural (EMF) and ethyl levulinate (EL) is an attractive biomass transformation due to the potential application in energy and chemical industry. Here, we report on the conversion with MOFs-based polyoxometalate [Cu-BTC][HPM] (NENU-5) as catalyst. The homogeneous distribution of HPM in the pores of Cu-BTC makes the composite combine the properties of catalytic activity of HPM and the insolubility, large surface and hierarchical pores of Cu-BTC. The catalyst demonstrates reusability and catalytic activity with 55% yield of EMF and 11% yield of EL.

Introduction

Currently, energy shortage and environmental pollution are still two major global problems. With the diminishing fossil fuel and growing demand for energy sources, it is very urgent to find reliable and renewable resources which can gradually replace fossil resources.[1-6]Biofuels, as extensive, abundant and low-cost renewable resources, have a great significance to reduce the excessive dependence on fossil resources, ease the energy crisis, decrease the environmental pollution, and promote the sustainable development of the whole human society.[7] A large number of research activities are carried out to turn biomass into liquid fuel and develop economically feasible methods on a industrial scale. Among the various desired platform chemicals, 5-hydroxymethylfurfural (HMF)derived from biomass is of central importance, because it can be converted into a series of high-quality fuels and high-value chemicals such as γ-valerolactone, levulinic acid, ethyl levulinate (EL), 2,5-dimethylfuran (DMF), 5-ethoxymethylfurfural (EMF) and so on due to its special structure with two functional groups combined with a furan ring.[8-13] Amongst, EMF has attracted much attention as a potential biofuel alternative because of its high energy density of 30.3 MJ/L, similar to diesel (33.6 MJ/L), and significantly higher than ethanol (23.5 MJ/L).[13] Meanwhile, the high oxidation stability of EMF can reduce the emission of soot, NOx and SOx.[14]In addition to EMF, EL, as a diluent for biodiesel fuels with high saturated fatty acid content, was investigated as a novel, bio-based cold flow improver for use in biodiesel fuels.[15]

In recent years, various acidic catalysts have been developed for the synthesis of EMF or EL. For instance, the etherification of HMF with ethanol is studied over a series of mesoporous silica catalysts and compared with the behavior of Brønsted acid H2SO4 and Amberlyst-15 by Lanzafame and co-workers.[12] Riisagar et al. developed a successive process to convert sugars to EMF and EL using sulfonic acid-functionalized ionic liquids.[16] The research group of Saha reported that direct transformation of sugarcane into a mixture of EMF and EL with 24% yield by Zr(O)Cl2/CrCl3 catalyst.[17] A variety of ionic liquids (imidazolium propane sulfonic acids) were synthesized by Guney et al. to transform of fructose into EMF of 55% yield and EL of 13% yield.[18] Heteropolyacid is also widely used for the conversion of biomass into biofuels[19] because of their Brønsted acidity, well defined structure, high proton mobility and the ability to accept and release electrons[20], such as the report about an EMF yield of 65% could be obtained in the presence of heteropolyacid H3PW12O40 under microwave heating.[21] Moreover, phosphomolybdic acid hydrate (HPM) used as catalyst in this reaction is rarely reported. In addition, the good solubility of heteropolyacid in most polar organic solvents and the relatively small surface areas result in the difficulty in the

[a.] Hefei National Laboratory for Physical Sciences at Microscale and Department of Materials Science & Engineering, University of Science and Technology of China, Hefei, China.
[b.] High Magnetic Field Laboratory, Hefei Institutes of Physical Science, Chinese Academy of Sciences, Hefei, Anhui 230031, P. R. China.
† Footnotes relating to the title and/or authors should appear here.
Electronic Supplementary Information (ESI) available: [details of any supplementary information available should be included here]. See DOI: 10.1039/x0xx00000x

recycle and performance of the catalyst. Therefore, it is strongly demanded to immobilize soluble acids on an insoluble support to transform stable and recyclable heterogeneous solid catalysts.

In recent decades, metal-organic frameworks (MOFs) have attracted much attention because of their special structure and widespread applications in gas storage and separation, catalysis, drug delivery and sensing.[22-24] The extra-large cavity and high surface area of MOFs make them ideal supports. Cu-BTC (BTC=benzene-1,3,5-tricarboxylate) which possess large surface area and suitable cavities with the proper size and shape can be used as host matrices for the encapsulation of HPM molecule[25] to form a insoluble and recyclable catalyst for biomass conversion. In the present work, we have examined the unique MOFs-based compound of [Cu-BTC][HPM] (NENU-5) for the direct conversion of HMF into EMF and EL in normal pressure condition. The composites combine the advantages of MOFs and POMs. It turned out that MOFs can provide adsorption sites for HPM to avoid HPM dissolving in solvents, making the catalysts recyclable.

Experimental

Preparation of the catalyst

All chemicals were commercially available and used without any purification. In a typical synthesis of NENU-5, Solution A: 200 mg of cupric acetate monohydrate, 0.5 mmol of L-lysine and 300mg of phosphomolybdicacid were dissolved in 40 ml deionized water under magnetic stirring to get a transparent solution. Solution B: 140 mg of 1,3,5-benzenetricarboxylic acid was dissolved in 40 ml ethanol under agitated stirring to get an absolute transparent solution. Solution B was poured into solution A to form green solution under continuous stirring. After stirring for 12 h, the resulting green precipitate was centrifuged and washed several times with ethanol before drying in an oven at 60 ℃.

HMF conversion into EMF and EL

In a typical experiment for the synthesis of EMF and EL from HMF, 0.5 mmol of HMF was dissolved in 4 ml of ethanol, 40 mg of catalyst was subsequently added. The mixture solution was transferred into a Teflon lined autoclave with a capacity of 10 mL and heated at reaction temperature for a period of time. After the reaction, the catalyst was removed by centrifugation and the yellow supernatant liquid was analyzed by Trace GC/ISQ MS. The yield of EMF and EL was quantified by GC-9860 from the calibration curve with dodecane as an internal standard.

Characterization of the catalyst

The powder X-ray diffraction (XRD) patterns were collected on Japan Rigaku D/MAX-cA X-ray diffractometer using Cu Kα radiation over the 2θ range of 5-65º, and the working voltage was 40 kV, the current was 200 mA. Scanning electron microscopy (SEM) images were performed on a JEOL JSM-6700M scanning electron microscope. High resolution transmission electron microscopy (HRTEM) and the distribution of element were characterized using the atomic

resolution analytical transmission electron microscopy (ARTEM, JEM-ARM200F) with energy dispersive X-ray (EDS, Oxford). The FTIR spectrum was determined using a Magna-IR 750 spectrometer. The specific surface area was evaluated at 77 K (Micromeritics ASAP 2020) using the Brunauer-Emmett-Teller method, while the pore volume and pore size were calculated according to the Barrett-Joyner-Halenda formula applied to the adsorption branch.

Results and discussion

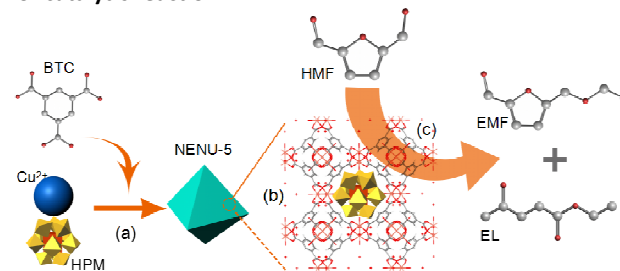### MOFs-supported phosphomolybdic acid synthesis strategy for catalytic reaction

Figure 1 Schematic illustration of the synthesis and catalysis procedure. (a) Synthesis of the catalyst. (b) The crystal structure of the catalyst. (c) The procedure of conversion of HMF into EMF and EL.

The overall synthesis route to prepare octahedral nanoparticles [Cu-BTC][HPM] with a formula of [Cu2(BTC)4/3(H2O)2]6[H3PMo12O40] (NENU-5)[26] as efficient catalyst for conversion of HMF into EMF and EL is illustrated in Fig. 1. The unique MOFs-based compound, which is based on Cu-based MOF (HKUST-1; Cu3(BTC)2(H2O)3; Cu-BTC) with Mo-based Keggin-type POMs (H3PMO12O40; HPM) periodically possessing the pores[25]. In this study, NENU-5 octahedron nanoparticles are synthesized by one-step co-precipitation method according to the literature[26]. The performance of [Cu-BTC][HPM] as catalyst for the conversion of HMF into EMF and EL is tested in a micro autoclave with ethanol as solvent.

Structural characterizations of catalyst

Typical SEM images of the [Cu-BTC][HPM] octahedral and slightly truncated octahedral with an average particle size of 700 nm are shown in Fig.2(a)(SEM). Fig.2(b) shows the XRD pattern of the catalyst before the catalyze which demonstrate the phase purity as well as the excellent crystallization of NENU-5 according to the reference [26,27]. For comparison, the XRD pattern of Cu-BTC prepared via the same method is also provided, which indicates the significant difference between [Cu-BTC][HPM] and Cu-BTC in diffraction pattern occurs especially in the 2θ range between 5 to 10 degrees. The disappearance of the (2 0 0) and (2 2 0) diffraction peaks between 5 to 10 degrees in Cu-BTC indicate HPM is not simply loaded on the surface of Cu-BTC. This variation is due to the HPM as guests have been introduced into the pores of Cu-BTC

Journal Name ARTICLE

as shown in Fig.1(b). The new structure change the original diffraction peaks of Cu-BTC. FTIR spectra of both Cu-BTC and [Cu-BTC][HPM] are shown in Fig.2(c). The FTIR spectrum of Cu-BTC displays the carboxylate stretch as three bands at 1619, 1442 and 1374 cm-1. The bands at 1707 and 1273 cm-1 correspond to the C=O and C-OH combination band of a carboxylic acid. The bands at 1112, 934 cm-1 and 760, 728 cm-1 in Cu-BTC are assigned to the C-H and C-C in BTC ring respectively.[28] Moreover, all characteristic stretching bands of HPM are present in the [Cu-BTC][HPM] spectra from 800 to 1100 cm-1 [29]. The strong stretching bands certify the existence of HPM.

Compared to the FTIR of HPM (Fig. S 1) with [Cu-BTC][HPM], a blue shift is observed for the typical Mo-O-Mo bands. Meanwhile, the bands corresponding to BTC ring are different between the FTIR of Cu-BTC and [Cu-BTC][HPM]. Take the molecular structure (Fig. 1(b)) into consideration, the above difference in FTIR suggests that there exists interactions between the BTC ring and Mo-O. There is no difference in the XRD and FTIR spectra after the catalytic reaction (Fig. 2(b, c)), which certify that the HPM is able to exist the pores of Cu-BTC steadily. Because of the interaction, the HPM act as template and the metal-organic framework is formed around the HPM to form a new molecular structure. The structure guarantee the stability of HPM with respect to leaching and other transformations, which are the essential properties of solid catalysts.
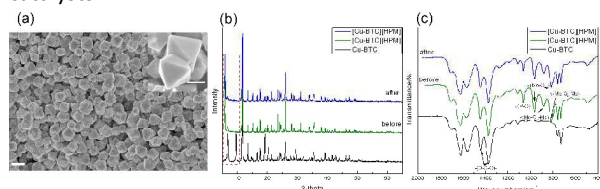

Figure 2 Characterization of the catalyst. (a) SEM image (inset: magnified image; scale bar, 500 nm) of the as-prepared [Cu-BTC][HPM] nano-octahedrons; scale bar, 1μm. (b) XRD patterns and (c) FTIR spectra of Cu-BTC and [Cu-BTC][HPM] before and after the catalytic reaction.

In order to further characterization of HPM distribution in Cu-BTC matrix, STEM and EDX mapping of the catalyst has been shown in Fig. 3. It is the top view of an octahedral nanoparticle in Fig.3 (a). As shown in Fig. 3 (b-d), the images of elemental mapping reveal that Cu, P and Mo atoms are uniformly distributed in a nanoparticle. It indicates that HPM are effectively incorporated into Cu-BTC matrix. Meanwhile, the nitrogen adsorption--desorption isotherm and the corresponding pore size distribution for both compounds of Cu-BTC and [Cu-BTC][HPM] were shown in Fig. S2. The BET surface area of [Cu-BTC][HPM] is 74m2/g, which is much smaller than Cu-BTC of 1373m2/g. The prodigious decrease in the surface area indicates that a large number of HPM occupys within the pores of the MOF material. Moreover, according to Fig. S2(b), the pore dimensions of Cu-BTC distribute intensively in 2nm. From Fig. S2(d), the pore size distribution

was reduced one order of magnitude than that of raw material due to plenty of HPM occupying the smaller pores of MOF material, which results in larger pores being remained in MOF material.
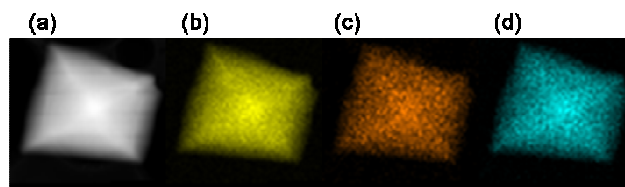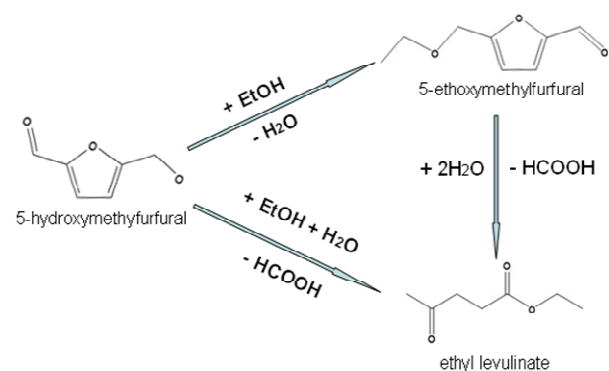

Figure 3 STEM and EDX mapping of the catalyst. (a) STEM of a [Cu-BTC][HPM] nanoparticle, elemental mapping of (b) Cu, (c) P and (d) Mo.

Catalytic performance for conversion of HMF into EMF and EL

Scheme 1 Conversion of HMF into EMF and EL in ethanol.

The conversion of HMF into EMF and EL is taken in a micro autoclave utilizing heat and autogenous pressure with ethanol as reactant and reaction medium[30]. A series of reaction systems using [Cu-BTC][HPM], Cu-BTC, HPM as catalysts as well as without a catalyst for the conversion are compared in the reaction condition of 100 $^{\circ}$C for 12 h. The main reaction products observed are 5-ethoxymethylfurfural (EMF) and ethyl levulinate (EL) (Fig. S3)[31]. EMF is derived from HMF etherification conversion, while EL formation is due to the reaction of HMF and further decomposition of EMF as shown in scheme 1[32]. When the reaction is carried out in the absence of a catalyst or using Cu-BTC as catalyst (Table 1, entry 1), no product is detected after the reaction, (Table 1, entry 3). However, no HMF is detected when [Cu-BTC][HPM] is used as catalyst which indicates the HMF complete reaction with 43.7% yield of EMF and 7.6% yield of EL (Table 1, entry 2). Taking the above results into consideration, HPM is the active catalytic species in [Cu-BTC][HPM] for the reaction. For comparison, the non-MOFs-based HPM is also employed to catalyze the reaction, and the amount of HPM is the same as the content of HPM in [Cu-BTC][HPM] according to ICP (Table S1). The yield of EMF and EL with HPM as the catalyst were close to those with [Cu-BTC][HPM] (Table 1, entry 4). However, unlike [Cu-BTC][HPM], HPM was soluble in ethanol and couldn't be reused.

Entry	Catalyst	Catalyst amount(m	HMF convers	EMF yield(%	EL yield

		g)	ion (%)	)	(%)
1	-	-	0	0	0
2	[Cu-BTC][HPM]	40	100	43.7	7.6
3	Cu-BTC	40	0	0	0
4	HPM	8.5	100	44.6	8.9

Table 1 Synthesis of EMF and EL from HMF catalyzed by various catalysts.

As shown in Fig.4, the reaction time and temperature had an effect on the yield of EMF and EL derived from HMF. Firstly, when the reaction was conducted at 100 ºC, the effect of different reaction time from 4h to 14h was investigated and illustrated in Fig.4(a). No HMF was detected in this group according to GC-MS, which indicates the HMF complete conversion at the reaction temperature of 100 ºC. Meanwhile, the main by-products in the reaction was 2-(diethoxymethyl)-5-(ethoxymethyl)furan (DEEF), which is difficult to be quantified because of no standard substance.(Fig. S4) EL yield was always rather low during the different time and the maximum was 7.9% at 14h. On the contrast, the reaction time had a remarkable effect on the yield of EMF. EMF yield increased from 11.4% for 4h to 43.7% for 12h, and then slightly declined to 40.8% for 14h, which may be due to the further decomposition of EMF. Overall, the total yield exhibited the same tendency as EMF yield and reached the maximum yield of 51.3% for 12h. At the optimum reaction time, the reaction was carried out at five different temperatures from 60 to 140 ºC. No products were detected at 60 ºC and only HMF was detected by GC-MS. It indicated the HMF cannot transform into EMF or EL at 60 ºC with [Cu-BTC][HPM] as catalyst. A little of HMF was detected in GC-MS at 80 ºC, while no HMF at higher temperatures. The effect of temperature on the yield of EMF and EL were very obvious.(Fig.4(b)) The yield of EMF and EL increased with the increasing of the reaction temperature from 80 to 140 ºC, same as the total yield. EMF and EL yield was largely increased from 10.7% and 3.0% at 80 ºC to maximal 68.4% and 20.2% at 140 ºC, respectively. The maximum total yield was close to 90%. The above results indicate EMF was the major product with a higher yield when [Cu-BTC][HPM] serves as catalyst. Meanwhile, the influence of the temperature on the reaction was greater than the time.
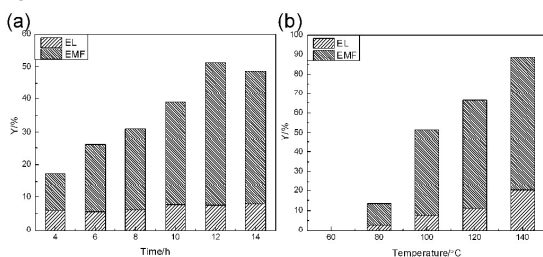

Figure 4 Influence of the time and temperature on the reaction. (a) Catalytic performance of the catalyst at 100 ºC for different reaction time. (b) Catalytic performance of the catalyst at 12 h for different reaction temperature.

Compared with HPM, a distinct advantage of using [Cu-BTC][HPM] as catalyst was that the procedure allows for convenient recycling of the catalyst, as [Cu-BTC][HPM] was insoluble in ethanol. Thus, the recycling experiments of [Cu-BTC][HPM] were carried out at 100 ºC for 12h. After the reaction, the catalyst could be readily collected by centrifugalization. The spent catalyst was then washed and dried, and reused for cycling tests. The steps were repeated five times and the result was shown in Fig.5. The total yield was almost the same, around 50%, in each run. However, the EMF yield decreased by 6.5% from first run to fifth run with the EL yield increased by 4.4%. In order to better understanding of the cycle performance of the material, the recycling experiments at a higher yield were also carried out and it's similar to the above results. (Fig. S5) Even though the EMF and EL yield couldn't be kept completely stable, the same total yield and insoluble still make [Cu-BTC][HPM] a alternative catalyst for the conversion of HMF into EMF and EL.
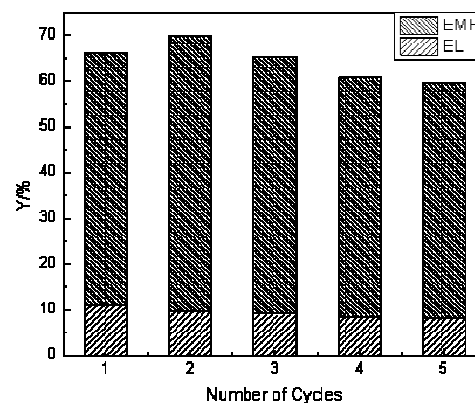

Figure 5 Catalyst recycling (Reaction conditions: 100 ºC for 12 h).

In this work, the MOFs-supported catalyst of [Cu-BTC][HPM] exhibits some unique advantages. In generally, MOFs-supported catalyst are synthesized by two steps at least, the synthesis of MOFs and then the load of the active component. The single-step strategy of [Cu-BTC][HPM] is facile and convenient, and more importantly, the active component of HPM have been introduced into the pores of MOFs and not just be deposited on the surface of MOFs. The HPM is uniformly distributed in a Cu-BTC nanoparticle matrix, which provides plenty of active sites in a nanoparticle. The structure with HPM being adsorbed in the molecular pores of Cu-BTC avoids the leaching of active component [25]. Meanwhile, the uniform mesoporosity and large surface of the MOFs-based material guarantee the plenty of reactant molecules enter into the pores and react under the assist of catalyst. Noteworthily the MOFs-based Keggin-type polyoxometalate materials don't apply to all MOFs. It depends on the shape and size of pores

which is suitable for polyoxometalate molecule. For example, according to the same method with different metal salts, the [M-BTC][HPM] (M=Zn, Co) were synthesized and tested for the HMF reaction. No products were detected and it indicate the peculiarity of [Cu-BTC][HPM].

In virtue of the unique structure, the [Cu-BTC][HPM] exhibits well activity for conversion of HMF into EMF and EL. EMF is always the major product at all reaction conditions, it indicate HPM is in favor of formation of EMF. Of course, as a by-product, EL is still important in energy＆environment and chemical industry. Both of reaction time and temperature affect the yield of EMF and EL. The maximum yield of EMF was at 140 ^{O}C, however, the catalyst couldn't keep absolute stable at the high temperature. A small amount of Cu was detected by XRD after the reaction (Fig. S6). Even under other conditions, the performance was also well compared with many catalysts (Table S2). Even if the catalytic performance is inferior to some other materials, it is due to the catalytic performance of HPM itself. The [Cu-BTC][HPM] which combine the catalytic activity of HPM and the insolubility of Cu-BTC can be reused. The catalyst still keeps considerable activity after five circulation. The XRD and FTIR of the catalyst (Fig.2(b) and (c)) after the reaction show no difference with the catalyst before the reaction. There is no change in the structure of the catalyst, and the HPM in the pores of Cu-BTC is not completely dissolved in ethanol according to ICP of the catalyst after the reaction (Table S1). It proves the superiority of the special structure of [Cu-BTC][HPM].

Conclusions

In summary, we report conversion of HMF into EMF and EL by the catalyst of MOFs-based polyoxometalate. The unique [Cu-BTC][HPM] (NENU-5) consisted of guest molecules of HPM occupied the biggest pores in Cu-BTC host, show the good catalytic activity in the conversion of HMF. Benefiting from the unique structure, the HPM can stably exist in the pores of the insoluble Cu-BTC, which make the catalyst reutilization. Moreover, such a strategy which introduces the soluble active component into the pores of insoluble MOFs could be applicable for biomass conversion.

Acknowledgements

Corresponding author

Qianwang Chen; Email:cqw@ustc.edu.cn

Notes and references

1   P. Gallezot, *Chem. Soc. Rev.*, **2012**, 41, 1538-1558.

2   L. L. Ma, T. J. Wang, Q. Y. Liu, X. H. Zhang, W. C. Ma, Q. A. Zhang, *Biotechnol. Adv.*, **2012**, 30, 859-873.

3   J. C. Serrano-Ruiz, R. Luque, A. Sepulveda-Escribano, *Chem.Soc. Rev.*, **2011**, 40, 5266-5281.

4   H. L. Long, X. B. Li, H. Wang, J. D. Jia, *Renewable Sustainable Energy Rev.*, **2013**, 26, 344-352.

5   G. Kocar, N. Civas, *Renewable Sustainable Energy Rev.*, **2013**, 28, 900-916.

6   J. H. Zhang, L. Lin, S. J. Liu, *Energy Fuels*, **2012**, 26, 4560-4567.

7   L. Hu, L. Lin, S. Liu, *Industrial & Engineering Chemistry Research*, **2014**, 53, 9969-9978.

8   Y. Román-Leshkov, C. J. Barrett, Z.Y. Liu, ,J. A. Dumesic, *Nature*, **2007**, 447, 982-985.

9   L. Deng, J. Li, D. M. Lai, Y. Fu, Q. X. Guo, *Angew. Chem. Int. Ed.*, **2009**, 48, 6529-6532.

10 J. Q. Bond, D. M. Alonso, D. Wang, R. M. West, J. A. Dumesic, *Science*, **2010**, 327, 1110-1114.

11 I. T. Horváth, H. Mehdi, V. Fábos, L. Boda, L. T. Mika, *Green Chemistry*, **2008**, 10, 238-242.

12 P. Lanzafame, D. M. Temi, S. Perathoner, *Catalysis today*, **2011**, 175, 435-441.

13 M. Mascal, E. B. Nikitin, *Angew. Chem. Int. Ed.*, **2008**, 47, 7924–7926.

14 G. J. M. Gruter, F. Dautzenberg,U.S. Patent Appl. 2011/0082304 A1, 2011

15 H. Joshi, B. R. Moser, J. Toler, *Biomass and bioenergy*, **2011**, 35, 3262-3266.

16 S. Saravanamurugan, O. Nguyen Van Buu, A. Riisager, *Chem. Sus. Chem.*, **2011**, 4, 723-726.

17 S. Dutta, S. De, Md. I. Alam, M. M. Abu-Omar, B. Saha, *J. Catal.*, **2012**, 288, 8–15.

18 G. A. Kraus, T. Guney, *Green Chemistry*, **2012**, 14, 1593-1596.

19 W. Deng, Q. Zhang, Y. Wang, *Dalton Transactions*, **2012**, 41, 9817-9831.

20 A. Bohre, S. Dutta, B. Saha, *ACS Sustainable Chemistry & Engineering*, **2015**, 3, 1263-1277.

21 Y. Yang ,M. M. Abu-Omar, C. Hu, *Applied Energy*, **2012**, 99, 80-84.

22 H. Furukawa, K. E. Cordova, M. O'Keeffe, O. M. Yaghi, *Science*, **2013**, 341, 1230444.

23 R. J. Kuppler, D. J. Timmons, Q. R. Fang, *Coord. Chem. Rev.*, **2009**, 253, 3042–3066.

24 S. L. James, *Chem. Soc. Rev.*, **2003**, 32, 276–288.

25 C. Y. Sun, *J. Am. Chem. Soc.*, **2009**, 131,1883–1888.

26 H. B. Wu, B. Y. Xia, L. Yu, *Nature communications*, **2015**, 6, 6512-6519.

27 M. Wilke, M. Klimakow, K. Rademann, *CrystEngComm*, 2016, 18, 1096-1100.

28 J. B. DeCoste, G. W. Peterson, B. J. Schindler, K. L. Killops, M. A. Browe, J. J. Mahle, *J. Mater. Chem. A*, **2013**, 1, 11922-11932.

29 G. R. Rao, T. Rajkumar, B. Varghese, *Solid State Sciences*, **2009**, 11, 36-42.

30 P. Lanzafame, K. Barbera, S. Perathoner, *J. Cat.*, **2015**, 330, 558-568.

31 R. Liu, J. Chen, X. Huang, *Green Chemistry*, **2013**, 15, 2895-2903.

32 T. Flannelly, S. Dooley, J. J. Leahy, *Energy & Fuels*, **2015**, 29, 7554-7565.

33 B. Liu, Z. Zhang, K. Huang. *Cellulose*, **2013**, 20, 2081-2089.

34 Y. Ren, B. Liu, Z. Zhang, *Journal of Industrial and Engineering Chemistry*, **2015**, 21, 1127-1131.

35 A. Liu, Z. Zhang, Z. Fang, *Journal of Industrial and Engineering Chemistry*, **2014**, 20, 1977-1984.

36 S. Wang , Z. Zhang , B. Liu, *Catalysis Science & Technology*, **2013**, 3, 2104-2112.

37 M. Mascal, E. B. Nikitin, *ChemSusChem*, **2009**, 2, 859-861.

38 S. Yin, J. Sun, B. Liu, *Journal of Materials Chemistry A*, **2015**, 3, 4992-4999.
39 B. Liu, Z. Gou, A. Liu, *Journal of Industrial and Engineering Chemistry*, **2015**, 21, 338-339.
40 A. Liu, B. Liu, Y. Wang, *Fuel*, **2014**, 117, 68-73.

Green Chemistry Accepted Manuscript